

# High-scan-range cryogenic scanning probe microscope

S. Urazhdin, I. J. Maasilta, S. Chakraborty, I. Moraru, and S. H. Tessmer<sup>a)</sup>  
*Department of Physics and Astronomy, Michigan State University, East Lansing, Michigan 48824*

(Received 31 May 2000; accepted for publication 27 June 2000)

We have designed and constructed a scanning probe microscope operable at temperatures down to 260 mK within a top-loading helium-3 cryostat. It achieves a large scan range with the sample situated near the bottom of the scanning head—maximizing the cooling efficiency of the liquid helium. The scan head is completely thermally compensated, thus eliminating thermal expansion and contraction on cooling and warm-up, as well as thermal drift during operation. We demonstrate the performance using two distinct scanning probe methods: scanning tunneling microscopy and charge accumulation imaging. © 2000 American Institute of Physics.  
[S0034-6748(00)03011-2]

## I. INTRODUCTION

A number of scanning-probe-microscopy-based techniques have been developed utilizing signals such as tunneling current, atomic force, and magnetic force to study surfaces.<sup>1</sup> Scanning tunneling microscopes (STM) typically need a high degree of stability to achieve atomic resolution topography and/or high-quality spectroscopy. The high stability and rigidity of the scanning head necessitate its small dimensions, leading to small scan ranges. On the other hand, experiments which probe mesoscopic phenomena<sup>2</sup> often require micron-scale scanning range as well as prolonged stable operation at cryogenic temperatures.

It can be challenging to construct piezoelectric-based microscopes compatible with cryogenic operation that achieve a high scan range. Simply incorporating long (5–10 cm) piezoelectric tubes into the popular Besocke design<sup>3</sup> results in a high position for the sample relative to the bottom of the scan head. This can make it difficult to efficiently use liquid helium to cool the sample. For example, in the direct immersion scheme, once the liquid level drops below the sample, its temperature begins to rise. It is generally advantageous to have the sample as close to the bottom of the microscope as possible—reducing the volume of undisturbed liquid below the sample.

One of the designs intended to solve this problem is shown in Fig. 1.<sup>4</sup> The sample holder is placed on three short carrier piezoelectric tubes used for the sample coarse positioning. An 8-cm-long scanning tube is situated above the sample to provide a large scan range. The drawback of this design is a lack of thermal compensation, as can be seen from Fig. 1. The contraction of the metal body upon cooling is of the order of 0.5 mm, much greater than that of the piezoelectric ceramic. This will lead to a crash unless extra precaution is taken. Moreover, even at the base temperature, minute thermal instabilities can lead to significant drift in tip-sample separation; fluctuations as small as 10 mK were found to cause nanometer-scale shifts.

## II. DESIGN

Our goal was to build a scanning head that combined large scanning range with complete thermal compensation. Moreover, we required dimensions sufficiently small to fit within the bore of a superconducting magnet (3.9 cm diameter) inside a top-loading commercial liquid helium-3 cryostat.<sup>5</sup> The main advantage of the top-loading probe is easy access to the scanning head and sample without the necessity of warming the cryostat. To achieve high cooling power and thermal stability, the tip and sample are immersed directly in liquid helium 3. We find that the He atmosphere is an inert environment comparable to high vacuum conditions.

A schematic of the design is shown in Fig. 2(a). The 7.6-cm-long piezo tubes are soldered to the top plate which is rigidly attached to the probe. The sample rests on the small feet that are part of cylindrical legs, as indicated in the figure. The legs are a central part of the design, shown in Fig. 2(b). A mechanism inside the legs allows the supporting feet to be rotated; by rotating each foot 180°, we open the space below the tip—permitting the sample holder to be loaded from the bottom. Each leg consists of a piston rigidly attached to the foot, and a small Be–Cu compression spring. The resulting upward pressure on the piston presses the supporting piece against the leg, without limiting its rotational motion. A groove made in the leg fixes the piece in two positions, directed inward or outward. As is evident from Fig. 2(a), the scanning head is thermally compensated; indeed, we find no significant change in tip-sample separation as the temperature varies from 300 K to 300 mK.

Figure 2(c) shows a bottom view of the assembly. The sample holder is similar in design to the Besocke ramps,<sup>6</sup> except that the sloped ramps and the sample are situated on opposite sides. We chose a slope of 2°, yielding a coarse vertical positioning range of 0.4 mm. Moreover, the sample sits on a positioning screw, that allows manual vertical positioning in the range of almost 1 cm. This is important in preventing the tip from being accidentally crashed during the insertion of the sample. In practice, the sample is typically 0.5 cm from the tip after initially inserting the sample holder. Of course, before we can turn the positioning screw to bring

<sup>a)</sup>Electronic mail: tessmer@pa.msu.edu

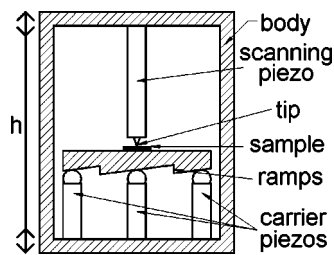


FIG. 1. Schematic of a microscope design utilized by a handful of experiments, including Ref. 4. The thermal-contraction mismatch between the metal body (hatched) and piezoelectric tubes represents a major drawback. Essentially, in response to temperature fluctuations, the body expands and contracts much more than the piezo ceramic. These uncompensated fluctuations in height  $h$  result in significant variations of the tip-sample separation.

it closer, the position of the ramps must be fixed. This is accomplished by pinching the sample holder from the sides using the three clamping screws, shown in Fig. 2(c). The clamping screws are attached to the brass displacer that also serves to screen electrical field generated by the operating piezo tubes. After the clamping screws are removed, an end cap is put in place. The interior of this cap provides a smooth surface for contact with the sides of the sample holder. We ensure low friction by applying  $\text{MoS}_2$  powder to the interior surface of the cap in addition to the sides and the ramps of the sample holder.

### III. OPERATION

The microscope is cooled by slowly lowering the probe into the cryostat—achieving a cooling rate of  $\sim 1$  K/min. There is little risk of mechanical vibrations causing a crash during this procedure, as gravity tends to pull the sample away from the tip. Finally, the fine sample approach is achieved by the standard inertial walking procedure utilized in Besocke-type designs.<sup>6</sup> We find our scanning piezo tube

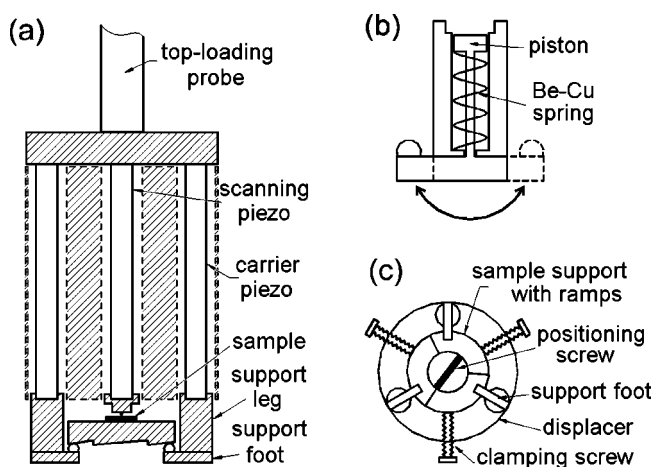


FIG. 2. (a) Schematic of scanning head. Both the tip and the sample are supported by identical piezoelectric tubes (dimensions: 7.6-cm-long $\times$ 4.8-mm-diam $\times$ 0.8 mm wall thickness). As a result the unit is nearly perfectly thermally compensated. The displacer, outlined in dashes, screens the tip from the electric fields of the piezo tubes. All the metal parts are made of brass, shown hatched. (b) Sketch of support leg showing the rotating foot assembly. (c) Bottom view of the microscope. The clamping screws fix the ramps to allow the positioning screw to be turned—the sample is attached to the other side of this screw. In this way, we can adjust the vertical position of the sample by as much as 1 cm. The diameter of the unit is 3.8 cm.

(7.6-cm-long $\times$ 4.8-mm-diam $\times$ 0.8 mm wall thickness) to have a sensitivity of 1300  $\text{\AA}/\text{V}$  laterally and 73  $\text{\AA}/\text{V}$  vertically at helium temperatures. Using commercially purchased electronics<sup>7</sup> which provide a voltage range of  $\pm 130$  V, we thus achieve an impressive cryogenic lateral scan range of 34  $\mu\text{m}$ . The same large range of motion of the carrier piezo tubes also enables us to do the fine sample approach very quickly. Typically, the full range of the ramps is traversed in approximately 2 min at helium temperatures.

We find the microscope to be sufficiently stable to function without a low-temperature vibration isolation stage. With regard to the entire cryostat, we have taken care to minimize building vibrations using a bungee cord suspension system. Mechanical pumps which are part of the cryogenic system represent a major source of additional vibrations. We have decoupled those modes by using tubing that has a section made of flexible rubber, connected to a section of stainless steel. That produces an impedance mismatch so that part of the vibrations are reflected at the junction.<sup>8</sup> We have also connected the tube rigidly to a heavy lead block at one point and immersed it into a sandbox at another.

The microscope has been designed to measure a variety of signals. Here we demonstrate operation for STM (tunneling mode) and for charge accumulation imaging (capacitance mode)—appropriate for semiconductor and insulating samples. Charge accumulation imaging<sup>4</sup> is a recently developed method—essentially a cryogenic form of scanning capacitance microscopy.<sup>9</sup> By monitoring the ac charge induced on a metal tip as a function of ac excitation voltage applied to the sample, we measure the local charge accumulating directly below the tip. A key component is a low-temperature charge sensor, originally developed for single-electron capacitance spectroscopy by Ashoori and co-workers.<sup>10</sup> This sensor is mounted directly to the scanning tube together with the tip. Utilizing low-input-capacitance high-electron-mobility transistors, the noise level for charge detection is  $\sim 0.004 e/\sqrt{\text{Hz}}$ . We operate the sensor at kilohertz frequency range, up to 100 kHz, limited by the lock-in amplifier used to measure the signal. The tip is kept a few nanometers above the surface of the sample so that no dc conduction between the sample and the tip takes place (no large dc bias voltage is applied); thus we only measure the capacitively induced charge. For samples that are uniformly good conductors, the measured signal simply equals the geometrical capacitance between the tip and sample. More interesting phenomena can be probed for samples that have regions that act as poor conductors. In these cases, the capacitance signal reflects the local resistivity and compressibility of the system. Moreover, the conducting layer can be buried within the sample below a dielectric surface, such as within a semiconductor heterostructure.

Figure 3(a) shows a 35  $\mu\text{m}\times$ 35  $\mu\text{m}$  topographic image of a platinum sample with a grid of 5  $\mu\text{m}\times$ 5  $\mu\text{m}$  pits that are 1800  $\text{\AA}$  deep, obtained in tunneling mode with the microscope at room temperature. The 35  $\mu\text{m}$  scan range is approximately the maximum range at helium temperatures. Figure 3(b) shows line scans across a single pit measured in both tunneling and capacitance modes. For the capacitance scan no feedback was used; the tip was simply scanned

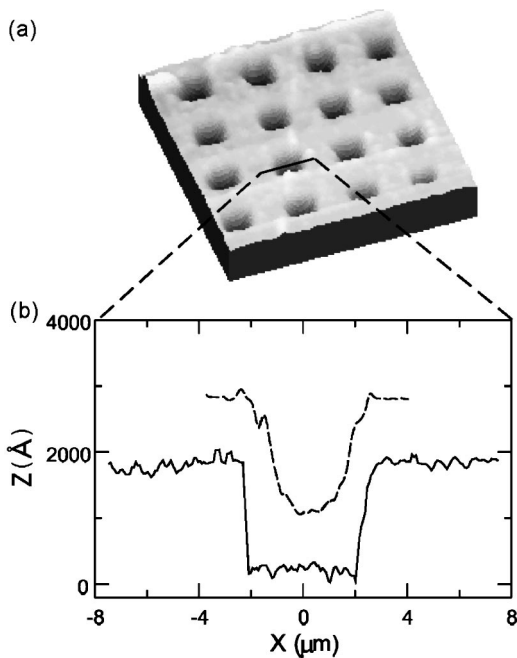


FIG. 3. (a) A  $35\ \mu\text{m} \times 35\ \mu\text{m}$  topographical image of a platinum sample with a grid of  $5\ \mu\text{m} \times 5\ \mu\text{m}$  pits that are 180 nm deep, obtained at room temperature. (b) Cross section across a single pit measured both in the tunneling mode (solid line) and in capacitance mode (dashed line).

above the sample in a straight line. The tunneling mode clearly has better resolution, comparing the sharpness of the walls. This is natural because tunneling takes place only at the apex of the tip on atomic scale, whereas the resolution in the capacitance mode is determined by distance between the tip and the sample and by the radius of curvature of the tip's apex,  $\sim 40$  nm for our chemically etched tips.<sup>11</sup> Nevertheless, Fig. 3(b) also shows that capacitance mode can give us more information than just the topography, even for simple metallic samples. As is clearly visible, capacitance has local maxima at the edges of the pits, as expected from electrostatics (electric field is higher around sharp corners).

Figures 4 and 5 demonstrate cryogenic operation using a GaAs–AlGaAs heterostructure sample containing a two-dimensional electron system (2DES) 60 nm below the surface. No direct electrical contact is made to the 2DES; instead we apply the ac excitation to a three-dimensional electrode 30 nm below the 2DES, separated by a tunneling barrier. The tip-sample approach is achieved in the tunneling mode, i.e., monitoring the tunneling current with the feedback loop on. It should be pointed out that this approach scheme works despite the 60-nm-thick insulating barrier between the tip and the 2DES. We find that a large bias voltage on the tip of +10 V sufficiently tilts the barrier to allow tunneling to surface states; tunneling current  $\sim 100$  pA can then be achieved. Hence, scanning the tip while using feedback to maintain a constant current yields the surface topography—just like standard STM. This vital information helps us to avoid tip-sample crashes for subsequent capacitance measurements, which are typically performed without feedback.

Figure 4(a) shows a tunneling mode image of the surface topography, taken at 4.2 K, with a cross section shown in

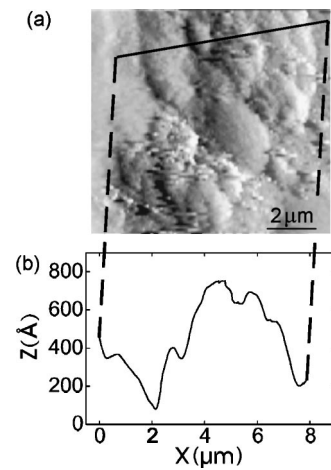


FIG. 4. (a) Topography of the GaAs surface of our heterostructure sample, measured at 4.2 K. To increase the contrast of the image, high pass filtering has been performed. (b) Cross section of the topography raw data, the location of which is shown in Fig. 5(a) by the line. The noise level is less than  $1\ \text{\AA}$  rms.

Fig. 4(b). As we see, the surface consists of elongated mounds of various sizes. Such features are typical of the epitaxially grown GaAs (001) surface, where the mounds tend to be elongated along the  $[\bar{1}10]$  direction.<sup>12</sup> With regard to capacitance measurements, so far we have implicitly assumed that the tip acts simply as a measuring device without perturbing the system. Indeed, the charge accumulation can be imaged noninvasively.<sup>4</sup> But we can also study how the tip can perturb the 2DES locally by applying a dc bias voltage. Figure 5 shows the signal as a function of the dc bias on the tip, at a temperature of 260 mK. As we decrease the tip voltage, the signal drops abruptly around  $-0.5$  V. This is the potential  $V_0$  where the 2DES becomes depleted locally, shown schematically as a black hole in Fig. 5 (inset). As indicated by the arrows, further decrease of the bias voltage causes the depleted hole to grow in size. The 15 aF magnitude of the step can be compared to a simple electrostatic model, where the step height is the difference in capacitance between a fully charged 2DES layer and the tip, and the locally depleted 2DES and the tip (capacitance to the back electrode). The comparison allows us to estimate the radius of the depletion hole at  $V_0$ . We find the radius to be roughly

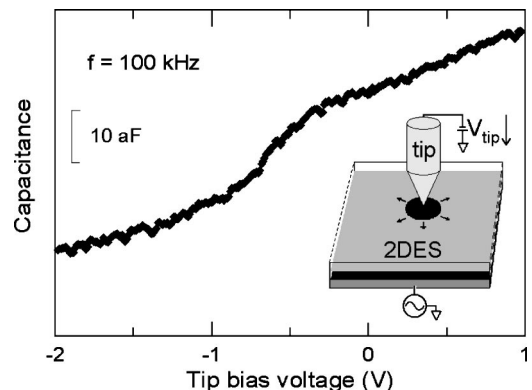


FIG. 5. Dependence of the capacitance signal on the tip dc bias voltage. The step feature marks the potential  $V_0$  where the 2DES becomes depleted locally. The data were acquired at 260 mK.

equal to the tip-2DES separation—consistent with numerical modeling of similar systems.<sup>13</sup>

In conclusion, we have constructed and tested a cryogenic scanning probe microscope operating at temperatures down to 260 mK. The design offers the following advantages: (i) It achieves an impressive scanning range (34  $\mu\text{m}$ ) at liquid helium temperatures, suitable for studies of mesoscopic samples. (ii) The stability of the design enables us to conduct experiments lasting for several days without significant drift of tip-sample separation, or lateral position of the tip. (iii) The microscope is fully thermally compensated, exhibiting no significant change in tip-sample separation upon cooling from room temperature to liquid helium temperatures.

#### ACKNOWLEDGMENTS

The authors gratefully acknowledge M. R. Melloch for providing the heterostructure sample, and E. J. Ertel and G. Heraty for valuable assistance. This work was supported by the National Science Foundation through the Division of Materials Research (DMR 9970756) and a seed grant from the MSU Center for Sensor Materials.

- <sup>1</sup>G. Binnig and H. Rohrer, *Rev. Mod. Phys.* **71**, S324 (1999).
- <sup>2</sup>Y. Imry, *Introduction to Mesoscopic Physics* (Oxford University Press, New York, 1997).
- <sup>3</sup>K. Besocke, *Surf. Sci.* **181**, 145 (1987).
- <sup>4</sup>S. H. Tessmer, P. I. Glicofridis, R. C. Ashoori, L. S. Levitov, and M. R. Melloch, *Nature (London)* **392**, 51 (1998).
- <sup>5</sup>Purchased from Oxford Instruments America, Inc., 130A Baker Avenue Extension, Concord, MA 01742, (978) 369-9933.
- <sup>6</sup>J. Frohn, J. F. Wolf, K. Besocke, and M. Teske, *Rev. Sci. Instrum.* **60**, 1200 (1989).
- <sup>7</sup>Purchased from RHK Technology, Inc., 1050 East Maple Road, Troy, MI 48083, (248) 577-5426.
- <sup>8</sup>R. Movshovich, in *Experimental Techniques in Condensed Matter Physics at Low Temperatures*, edited by R. C. Richardson and E. N. Smith (Addison-Wesley, New York, 1988), Sec. 3.3.
- <sup>9</sup>C. C. Williams, W. P. Hough, and S. A. Rishton, *Appl. Phys. Lett.* **55**, 203 (1989).
- <sup>10</sup>R. C. Ashoori, H. L. Stormer, J. S. Weiner, L. N. Pfeiffer, S. J. Pearton, K. W. Baldwin, and K. W. West, *Phys. Rev. Lett.* **68**, 3088 (1992).
- <sup>11</sup>Purchased from Materials Analytical Services, 616 Hutton Street, Suite 101, Raleigh, NC 27606, (919) 829-7041.
- <sup>12</sup>J. Sudijono, M. D. Johnson, C. W. Snyder, M. B. Elowitz, and B. G. Orr, *Phys. Rev. Lett.* **69**, 2811 (1992).
- <sup>13</sup>M. A. Eriksson, R. G. Beck, M. Topinka, J. A. Katine, R. M. Westervelt, K. L. Campman, and A. C. Gossard, *Appl. Phys. Lett.* **69**, 671 (1996).